Supplementary information

Atmospheric Oxidation of Fenthion initiated by Hydroxyl Radical and Ozone

Table S1. Relative energy, enthalpy and free energy corresponding to the reactive species involved in the H-abstraction reactions of fenthion initiated by •OH calculated at M06-2X/6-311++G(d,p) and ωb97X-D/6-311++G(d,p) level of theory.

Table S2. Relative energy, enthalpy and free energy corresponding to the reactive species involved in the •OH-addition reactions of fenthion calculated at M06-2X/6-311++G(d,p) and ωb97X-D/6-311++G(d,p) level of theory.

Table S3. Calculated rate constants (k, cm^3 $molecule^{-1}$ s^{-1}) and the total rate constant (k_{total}, cm^3 $molecule^{-1}$ s^{-1}) for the studied •OH initiated reactions of fenthion over the temperature range 200 – 400 K.

Table S4. Relative energy, enthalpy and free energy corresponding to the reactive species involved in the studied subsequent reactions of the intermediates, IM19 and IM20 calculated at M06-2X/6-311++G(d,p) level of theory.

Table S5: The maximum absorbance wavelength, excitation energy, electronic transition and oscillator strength of fenthion and its products calculated at TD-M06-2X/6-311++G(d,p) level of theory.

Table S6. Relative energy, enthalpy and free energy corresponding to the reactive species involved in the O_3 initiated reactions of fenthion calculated at M06-2X/6-311++G(d,p) level of theory.

Table S7. Calculated rate constants (k, cm^3 $molecule^{-1}$ s^{-1}) and the total rate constant (k_{total}, cm^3 $molecule^{-1}$ s^{-1}) for the studied •O_3 initiated reactions of fenthion over the temperature range 200 – 400 K.

Figure S1. The IRC plots for the •OH initiated reactions of fenthion calculated at M06-2X/6-311++G(d,p) level of theory.

Figure S2. The geometry of reactive species involved in the H abstraction reaction of fenthion initiated by •OH optimized at M06-2X/6-311++G(d,p) level of theory.

Figure S3. The geometry of reactive species involved in the •OH-addition reactions of fenthion optimized at M06-2X/6-311++G(d,p) level of theory.

Figure S4. Time-dependent species population profiles for the reaction pathway R1 at 298 K, calculated at different pressures (P) using MESMER software employing RRKM theory.

Figure S5. The geometry of reactive species involved in the O_3 initiated reactions of fenthion optimized at M06-2X/6-311++G(d,p) level of theory.

Table S1. Relative energy (ΔE), enthalpy (ΔH_{298}) and free energy (ΔG_{298}) corresponding to the reactive species involved in the H-abstraction reactions of fenthion initiated by •OH calculated at M06-2X/6-311++G(d,p) and ωb97X-D/6-311++G(d,p) level of theory. The energy is given in kcal/mol. (For reaction labels refer Scheme 1)

Reaction pathway	Reactive species	H-abstraction					
		M06-2X/6-311++G(d,p)			ωb97X-D/6-311++G(d,p)		
		ΔE	ΔH_{298}	ΔG_{298}	ΔE	ΔH_{298}	ΔG_{298}
R1	RC1	-8.6	-9.1	-0.7	-9.5	-10.1	-1.4
	TS1	2.1	1.5	10.6	0.6	0.1	8.7
	IC1	-12.5	-12.3	-5.3	-10.0	-9.8	-3.4
	IM1+H_2O	-7.8	-7.6	-9.0	-9.5	-10.1	-10.0
R2	RC2	-5.1	-5.9	4.0	-4.8	-5.2	2.9
	TS2	2.4	1.6	11.4	0.7	-0.1	9.7
	IC2	-10.1	-10.5	-1.5	-8.3	-8.1	-1.2
	IM2+ H_2O	-4.3	-4.0	-5.3	-1.5	-1.1	-3.3
R3	RC3	-7.6	-7.9	0.7	-6.9	-7.3	1.0
	TS3	0.6	-0.3	10.1	-0.9	-1.6	8.3
	IC3	-11.7	-11.6	-3.6	-8.4	-8.4	-0.8
	IM3+ H_2O	-4.9	-4.6	-6.0	-3.7	-3.3	-5.2
R4	RC4	-6.5	-6.7	1.0	-5.0	-5.2	2.8
	TS4	-1.6	-2.5	6.8	-2.5	-3.3	5.4
	IC4	-25.7	-25.5	-19.1	-25.8	-25.6	-19.4
	IM4+ H_2O	-22.2	-22.0	-23.2	-22.3	-22.0	-23.5
R5	RC5	-4.9	-5.3	3.0	-4.2	-4.5	3.0
	TS5	-0.6	-1.6	8.1	-2.7	-3.6	5.7
	IC5	-30.2	-30.1	-23.5	-30.6	-30.6	-23.4
	IM5+ H_2O	-26.4	-26.4	-27.1	-26.8	-26.7	-27.6
R6	RC6	-5.1	-5.9	3.9	-4.8	-5.2	2.9
	TS6	2.9	2.2	9.9	2.8	3.9	7.6
	IC6	-21.5	-21.4	-14.0	-21.6	-21.5	-13.9
	IM6+ H_2O	-17.0	-16.7	-18.1	-17.2	-16.9	-18.3

Table S2. Relative energy (ΔE), enthalpy (ΔH_{298}) and free energy (ΔG_{298}) corresponding to the reactive species involved in the •OH-addition reactions of fenthion calculated at M06-2X/6-311++G(d,p) and ωb97X-D/6-311++G(d,p) level of theory. (For reaction labels refer Scheme 2)

Reaction pathway	Reactive species	•OH -addition					
		M06-2X/6-311++G(d,p)			ωb97X-D/6-311++G(d,p)		
		ΔE	ΔH_{298}	ΔG_{298}	ΔE	ΔH_{298}	ΔG_{298}
R7	RC7	-8.8	-9.2	-0.1	-6.9	-7.3	1.1
	TS7	-1.1	-2.2	8.7	-2.5	-3.4	6.8
	IM7	-21	-23	-11	-21.3	-22.5	-12.1
R8	RC8	-8.8	-9.2	-0.1	-6.9	-7.3	1.1
	TS8	0.56	-0.5	9.8	-0.6	-1.7	8.7
	IM8	-20	-21	-10	-19.4	-20.4	-10.5
R9	RC9	-8.8	-9.2	-0.1	-6.8	-7.0	0.1
	TS9	-0.4	-1.5	9.1	-2.4	-3.4	6.8
	IM9	-18	-19	-9.1	-18.4	-19.5	-9.3
R10	RC10	-8.3	-8.6	0	-6.6	-6.9	1.7
	TS10	-2.3	-3.3	7.4	-3.6	-4.6	6.1
	IM10	-20	-22	-10	-20.4	-21.6	-10.3
R11	RC11	-8.3	-8.6	0	-6.9	-7.3	1.0
	TS11	0.42	-0.7	11	-0.7	-0.7	8.2
	IM11	-24	-26	-14	-21.8	-22.9	-12.0
R12	RC12	-8.8	-9.2	-0.1	-7.6	-7.0	1.8
	TS12	-2.9	-4	7.1	-4.7	-5.7	5.2
	IM12	-22	-23	-11	-21.8	-22.9	-12.0
R13	RC13	-4.7	-4.7	1.9	-3.8	-3.9	3.5
	TS13	1.48	0.57	10	-0.4	-1.3	8.4
	IM13	-22	-24	-13	-21.7	-22.9	-12.4
R14	RC14	-4.9	-4.7	1.3	-3.4	-3.2	2.8
	TS14	0.32	-0.6	9.5	-1.1	-1.9	7.8
	IM14	-24	-25	-15	-23.5	-24.5	-14.3
R15	RC15	-4.9	-5.3	3	-3.1	-3.0	3.2
	TS15	2.17	1.33	11	-0.1	-0.8	8.4
	IM15	-17	-18	-7.6	-17.6	-18.7	-8.7
R16	RC16	-5	-5.3	1.9	-3.7	-4.0	3.6
	TS16	1.54	0.62	11	-0.4	-1.3	8.9
	IM16	-19	-20	-9.2	-19.2	-20.3	-9.4
R17	RC17	-4.7	-4.7	1.9	-3.8	-3.9	3.5
	TS17	3.39	2.59	12	1.6	0.8	10.2
	IM17	-22	-24	-12	-22.3	-23.3	-12.5
R18	RC18	-4.7	-4.7	1.9	-3.8	-3.9	3.5
	TS18	-0.2	-1	8.4	-2.6	-3.3	5.9
	IM18	-19	-20	-10	-19.7	-20.7	-10.7
R19	RC19	-7.2	-7.4	0.7	-6.9	-7.4	1.8
	TS19	-5.7	-6.6	3.4	-5.3	-6.5	4.0
	IM19	-21	-23	-11	-18.6	-19.9	-8.4
R20	RC20	-7.3	-7.7	1.6	-6.8	-7.3	1.9
	TS20	-5.6	-6.9	4	-5.3	-6.6	4.2
	IM20	-16	-18	-5.9	-14.3	-15.5	-4.7

Table S3. Calculated rate constants (k, cm^3 $molecule^{-1}$ s^{-1}) and the total rate constant (k_{total}, cm^3 $molecule^{-1}$ s^{-1}) for the studied •OH initiated reactions of fenthion over the temperature range 200 – 400 K.

Reaction Pathway	k ($cm^3molecule^{-1}s^{-1}$)					
	200 K	**250 K**	**298 K**	**300 K**	**350 K**	**400 K**
R1	$5.3x10^{-14}$	$5.7x10^{-14}$	$6.4x10^{-14}$	$6.5x10^{-14}$	$7.5x10^{-14}$	$8.7x10^{-14}$
R2	$1.1x10^{-15}$	$1.2x10^{-15}$	$1.3x10^{-15}$	$1.3x10^{-15}$	$1.5x10^{-15}$	$1.8x10^{-15}$
R3	$9.3x10^{-15}$	$9.7x10^{-15}$	$1.0x10^{-14}$	$1.0x10^{-14}$	$1.2x10^{-14}$	$1.4x10^{-14}$
R4	$3.3x10^{-12}$	$2.1x10^{-12}$	$1.6x10^{-12}$	$1.6x10^{-12}$	$1.3x10^{-12}$	$1.2x10^{-12}$
R5	$3.0x10^{-17}$	$3.9x10^{-17}$	$4.9x10^{-17}$	$5.0x10^{-17}$	$6.2x10^{-17}$	$7.7x10^{-17}$
R6	$4.1x10^{-13}$	$5.1x10^{-13}$	$6.2x10^{-13}$	$6.2x10^{-13}$	$7.5x10^{-13}$	$9.0x10^{-13}$
R7	$3.9x10^{-16}$	$1.7x10^{-16}$	$1.1x10^{-16}$	$1.1x10^{-16}$	$8.3x10^{-17}$	$7.0x10^{-17}$
R8	$1.2x10^{-14}$	$1.2x10^{-14}$	$1.2x10^{-14}$	$1.2x10^{-14}$	$1.3x10^{-14}$	$1.4x10^{-14}$
R9	$1.3x10^{-13}$	$1.1x10^{-13}$	$1.0x10^{-13}$	$9.9x10^{-14}$	$9.6x10^{-14}$	$9.7x10^{-14}$
R10	$1.1x10^{-11}$	$3.5x10^{-12}$	$1.7x10^{-12}$	$1.7x10^{-12}$	$1.0x10^{-12}$	$7.8x10^{-13}$
R11	$6.9x10^{-15}$	$6.4x10^{-15}$	$6.5x10^{-15}$	$6.5x10^{-15}$	$6.9x10^{-15}$	$7.5x10^{-15}$
R12	$3.1x10^{-11}$	$7.1x10^{-12}$	$2.8x10^{-12}$	$2.7x10^{-12}$	$1.4x10^{-12}$	$9.2x10^{-13}$
R13	$7.9x10^{-17}$	$6.8x10^{-17}$	$6.7x10^{-17}$	$6.7x10^{-17}$	$7.1x10^{-17}$	$7.8x10^{-17}$
R14	$1.7x10^{-14}$	$1.8x10^{-14}$	$2.0x10^{-14}$	$2.0x10^{-14}$	$2.3x10^{-14}$	$2.6x10^{-14}$
R15	$2.9x10^{-14}$	$3.1x10^{-14}$	$3.3x10^{-14}$	$3.3x10^{-14}$	$3.7x10^{-14}$	$4.1x10^{-14}$
R16	$1.7x10^{-14}$	$1.7x10^{-14}$	$1.8x10^{-14}$	$1.8x10^{-14}$	$2.0x10^{-14}$	$2.2x10^{-14}$
R17	$3.2x10^{-15}$	$2.4x10^{-15}$	$2.2x10^{-15}$	$2.2x10^{-15}$	$2.0x10^{-15}$	$2.1x10^{-15}$
R18	$3.3x10^{-13}$	$3.3x10^{-13}$	$3.4x10^{-13}$	$3.4x10^{-13}$	$3.6x10^{-13}$	$4.0x10^{-13}$
R19	$1.6x10^{-7}$	$9.8x10^{-9}$	$1.6x10^{-9}$	$1.5x10^{-9}$	$4.3x10^{-10}$	$1.6x10^{-10}$
R20	$7.5x10^{-8}$	$3.9x10^{-9}$	$6.0x10^{-10}$	$5.6x10^{-10}$	$1.4x10^{-10}$	$5.5x10^{-11}$
k_{total}	**$2.4x10^{-7}$**	**$1.3x10^{-8}$**	**$2.2x10^{-9}$**	**$2.1x10^{-9}$**	**$5.9x10^{-10}$**	**$2.2x10^{-10}$**

Table S4. Relative energy (ΔE), enthalpy (ΔH_{298}) and free energy (ΔG_{298}) corresponding to the reactive species involved in the studied subsequent reactions of the intermediates, IM19

Reaction pathway	Reactive species	ΔE	ΔH_{298}	ΔG_{298}
R19a	**IM19**	0	0	0
	P1	-64.4	-65.6	-54.0
R21a	**IM19**	0	0	0
	RC21a	-21.3	-22.7	-11.0
	TS21a	-15.7	-17.0	-5.5
	IC21a	-37.7	-38.7	-27.2
	IM21+P3	-28.8	-30.1	-30.9
R19b	**IM19+O_2**	0	0	0
	RC19b	-3.1	-2.8	5.5
	TS19b	6.7	6.1	16.9
	IM19b	0.5	-0.1	10.6
R19b1	**IM19+O_2**	0	0	0
	TS19b1	0.6	-0.3	10.6
	IC19b1	-32.7	-32.8	-35.1
	P5+SOOH	-19.4	-19.5	-22.8
R20a	**IM20**	0	0	0
	P2	-67.4	-68.7	-56.9
R21b	**IM20**	0	0	0
	RC21b	-18.6	-19.9	-8.3
	TS21b	-14.1	-15.5	-4.0
	IC21b	-40.5	-41.5	-31.9
	IM21+P3	-27.9	-29.2	-29.9
R20b	**IM20+ O_2**	0	0	0
	RC20b	-1.7	-1.3	5.8
	TS20b	6.2	5.5	16.3
	IM20b	-0.2	-0.9	10.2
R20b1	**IM20+ O_2**	0	0	0
	TS20b1	-9.9	-11.0	1.4
	IC20b1	-30.6	-30.0	-32.1
	P6+SOOH	-24.8	-24.9	-28.0
R22	**IM21+HO_2•**	0	0	0
	RC22	-12.6	-12.7	-3.2
	TS22	-11.2	-11.7	-1.0
	IC22	-43.5	-42.9	-35.5
	P4+ O_2	-40.4	-40.3	-39.2

and IM20 calculated at M06-2X/6-311++G(d,p) level of theory. (For reaction labels refer Scheme 3)

Table S5: The maximum absorbance wavelength (λ_{max} in nm), excitation energy (T_v in eV), electronic transition and oscillator strength (f in a.u) of fenthion and its products calculated at TD-M06-2X/6-311++G(d,p) level of theory.

Reactive species	λ_{max}	T_v	Electronic transition	f
Fenthion	209	5.93	H-1 → L+1	0.12
P1	222	5.57	H → L+4	0.34
P2	220	5.63	H-1 → L+2	0.17
P3	216	5.72	H → L+4	0.19
P4	202	6.12	H-1 → L	0.07
P5	211	5.85	H-2 → L+2	0.18
P6	210	5.90	H-1 → L+1	0.11

Table S6. Relative energy (ΔE), enthalpy (ΔH_{298}) and free energy (ΔG_{298}) corresponding to the reactive species involved in the O_3 initiated reactions of fenthion calculated at M06-2X/6-311++G(d,p) level of theory. (For reaction labels refer Discussions in Page no. 13 of the main manuscript)

Reaction pathway	Reactive species	O_3 -addition		
		ΔE	**ΔH_{298}**	**ΔG_{298}**
S1FE	**ORC1**	-7.1	-6.7	3.9
	OTS1	5.5	4.8	18.8
	PO1	-39.2	-40.3	-25.6
S1FX	**ORC2**	-6.4	-6.1	5.0
	OTS2	7.9	7.2	21.2
	PO2	-38.7	-39.9	-25.3
S1BE	**ORC3**	-5.4	-4.9	3.7
	OTS3	6.4	5.6	19.6
	PO3	-37.9	-39.0	-24.4
S1BX	**ORC4**	-4.4	-3.9	5.4
	OTS4	8.5	7.8	21.7
	PO4	-37.3	-38.4	-24.0
S2FE	**ORC5**	-8.1	-8.0	3.6
	OTS5	4.6	3.8	18.7
	PO5	-35.7	-36.9	-21.6
S2FX	**ORC6**	-9.1	-9.2	3.6
	OTS6	5.9	5.0	19.8

	PO6	-36.7	-38.0	-22.7
S2BE	**ORC7**	-5.3	-4.8	4.2
	OTS7	7.1	6.5	19.5
	PO7	-37.1	-38.4	-23.3
S2BX	**ORC8**	-4.8	-4.4	4.9
	OTS8	9.9	9.2	22.8
	PO8	-38.6	-39.9	-24.1
S3FE	**ORC9**	-8.1	-8.0	3.6
	OTS9	3.7	2.8	17.7
	PO9	-38.6	-39.7	-24.7
S3FX	**ORC10**	-9.1	-9.2	3.6
	OTS10	5.3	4.2	20.3
	PO10	-39.5	-40.6	-25.5
S3BE	**ORC11**	-5.4	-4.9	4.3
	OTS11	7.4	6.8	20.3
	PO11	-38.3	-39.3	-25.9
S3BX	**ORC12**	-8.5	-8.4	2.9
	OTS12	9.1	8.5	21.4
	PO12	-40.5	-42.1	-25.1
S4FE	**ORC13**	-7.1	-6.9	4.6
	OTS13	5.4	4.6	19.4
	PO13	-38.3	-39.4	-24.8
S4FX	**ORC14**	-7.4	-7.1	3.7
	OTS14	8.5	7.9	21.8
	PO14	-37.5	-38.5	-23.5
S4BE	**ORC15**	-5.0	-4.4	3.8
	OTS15	8.1	7.5	20.3
	PO15	-35.7	-36.7	-22.7
S4BX	**ORC16**	-3.8	-3.2	5.7
	OTS16	10.6	10.0	23.2
	PO16	-34.6	-35.5	-22.0
S5FE	**ORC17**	-5.0	-4.6	5.4
	OTS17	9.0	8.4	21.8
	PO17	-36.2	-37.1	-22.8
S5FX	**ORC18**	-5.2	-4.7	5.4
	OTS18	10.5	9.9	23.9
	PO18	-38.8	-39.8	-25.4
S5BE	**ORC19**	-5.4	-4.9	4.3
	OTS19	9.2	8.6	22.0
	PO19	-36.9	-38.0	-22.8
S5BX	**ORC20**	-5.0	-4.5	4.4
	OTS20	10.7	10.1	22.4

	PO20	-40.5	-41.6	-26.5
S6FE	**ORC21**	-7.2	-6.9	4.6
	OTS21	6.4	5.6	20.6
	PO21	-39.4	-40.6	-24.7
S6FX	**ORC22**	-7.7	-7.4	4.1
	OTS22	10.3	9.5	24.5
	PO22	-40.4	-41.6	-25.8
S6BE	**ORC23**	-5.5	-5.0	3.6
	OTS23	8.0	7.4	21.0
	PO23	-40.3	-41.3	-26.9
S6BX	**ORC24**	-5.4	-4.9	4.5
	OTS24	9.7	9.1	22.5
	PO24	-43.4	-44.5	-29.5
S7PS	**ORC25**	-5.4	-5.1	5.1
	OTS25	4.9	4.2	18.2
	PO25	-28.5	-29.6	-14.4

Table S7. Calculated rate constants (k, cm^3 $molecule^{-1}$ s^{-1}) and the total rate constant (k_{total}, cm^3 $molecule^{-1}$ s^{-1}) for the studied $\bullet O_3$ initiated reactions of fenthion over the temperature range 200 – 400 K.

Reaction Pathway	k ($cm^3molecule^{-1}s^{-1}$)					
	200 K	**250 K**	**298 K**	**300 K**	**350 K**	**400 K**
S1FE	1.34×10^{-21}	1.04×10^{-20}	4.07×10^{-20}	4.28×10^{-20}	4.51×10^{-20}	1.38×10^{-19}
S1FX	3.07×10^{-24}	7.99×10^{-23}	6.65×10^{-22}	7.20×10^{-22}	7.78×10^{-22}	4.27×10^{-21}
S1BE	1.91×10^{-22}	2.25×10^{-21}	1.14×10^{-20}	1.21×10^{-20}	1.28×10^{-20}	4.77×10^{-20}
S1BX	7.33×10^{-25}	2.59×10^{-23}	2.60×10^{-22}	2.84×10^{-22}	3.09×10^{-22}	1.95×10^{-21}
S2FE	5.11×10^{-21}	2.21×10^{-20}	6.04×10^{-20}	6.27×10^{-20}	6.52×10^{-20}	1.52×10^{-19}
S2FX	1.78×10^{-22}	1.06×10^{-21}	3.49×10^{-21}	3.65×10^{-21}	3.82×10^{-21}	1.03×10^{-20}
S2BE	1.12×10^{-22}	3.98×10^{-22}	2.56×10^{-21}	2.75×10^{-21}	2.94×10^{-21}	1.33×10^{-20}
S2BX	3.55×10^{-26}	2.52×10^{-24}	3.93×10^{-23}	4.35×10^{-23}	4.81×10^{-23}	4.27×10^{-22}
S3FE	5.53×10^{-20}	1.54×10^{-19}	3.17×10^{-19}	3.26×10^{-19}	3.36×10^{-19}	6.31×10^{-19}
S3FX	1.78×10^{-22}	1.06×10^{-21}	3.49×10^{-21}	3.65×10^{-21}	3.82×10^{-21}	1.03×10^{-20}
S3BE	2.31×10^{-23}	4.80×10^{-22}	3.46×10^{-21}	3.73×10^{-21}	4.01×10^{-21}	1.97×10^{-20}
S3BX	6.99×10^{-25}	3.62×10^{-23}	4.62×10^{-22}	1.42×10^{-22}	1.55×10^{-22}	1.16×10^{-21}
S4FE	6.18×10^{-22}	4.41×10^{-21}	1.63×10^{-20}	1.71×10^{-20}	1.80×10^{-20}	5.27×10^{-20}
S4FX	6.57×10^{-25}	2.39×10^{-23}	2.44×10^{-22}	2.66×10^{-22}	2.90×10^{-22}	1.86×10^{-21}
S4BE	1.08×10^{-23}	3.34×10^{-22}	9.53×10^{-22}	1.03×10^{-21}	1.12×10^{-21}	6.53×10^{-21}
S4BX	1.21×10^{-26}	1.27×10^{-24}	2.51×10^{-23}	2.81×10^{-23}	3.13×10^{-23}	3.34×10^{-22}
S5FE	1.80×10^{-26}	8.01×10^{-25}	9.51×10^{-24}	1.04×10^{-23}	1.14×10^{-23}	8.40×10^{-23}
S5FX	3.39×10^{-27}	3.40×10^{-25}	6.59×10^{-24}	7.36×10^{-24}	8.20×10^{-24}	8.65×10^{-23}
S5BE	2.53×10^{-25}	1.33×10^{-23}	1.71×10^{-22}	1.89×10^{-22}	2.07×10^{-22}	1.59×10^{-21}
S5BX	3.28×10^{-27}	3.55×10^{-25}	7.21×10^{-24}	8.06×10^{-24}	9.00×10^{-24}	9.81×10^{-23}
S6FE	4.05×10^{-23}	4.40×10^{-22}	2.12×10^{-21}	2.25×10^{-21}	2.39×10^{-21}	8.63×10^{-21}
S6FX	1.81×10^{-27}	1.49×10^{-25}	2.53×10^{-24}	2.81×10^{-24}	3.12×10^{-24}	2.98×10^{-23}
S6BE	3.91×10^{-24}	1.12×10^{-22}	9.86×10^{-22}	1.07×10^{-21}	1.16×10^{-21}	6.63×10^{-21}
S6BX	6.53×10^{-26}	4.36×10^{-24}	6.56×10^{-23}	7.26×10^{-23}	8.02×10^{-23}	6.93×10^{-22}
PS	3.55×10^{-18}	5.79×10^{-18}	8.46×10^{-18}	8.59×10^{-18}	8.72×10^{-18}	1.25×10^{-17}
k_{total}	3.61×10^{-18}	5.99×10^{-18}	8.92×10^{-18}	9.07×10^{-18}	9.22×10^{-18}	1.36×10^{-18}

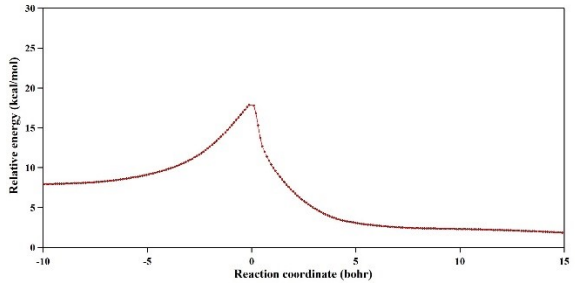

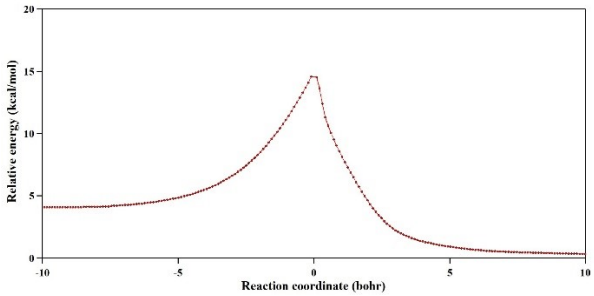

R1

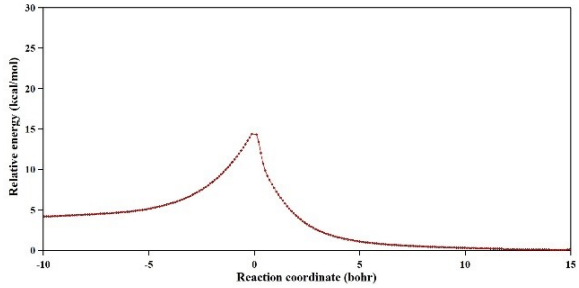

R2

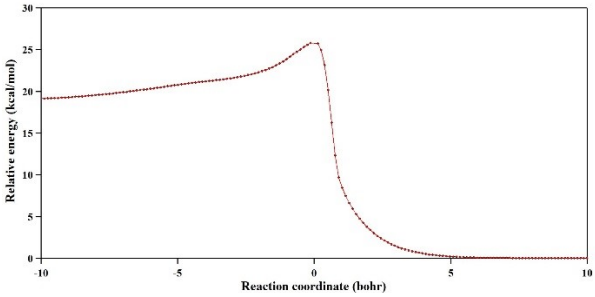

R3

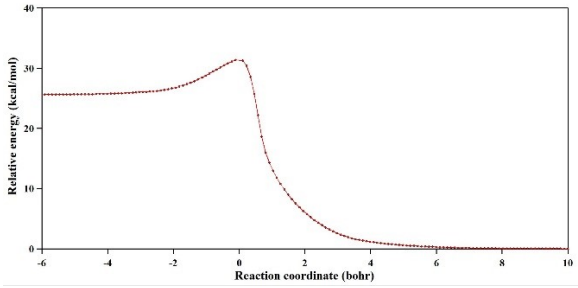

R4

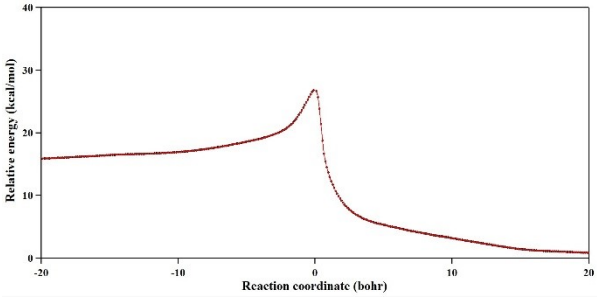

R5

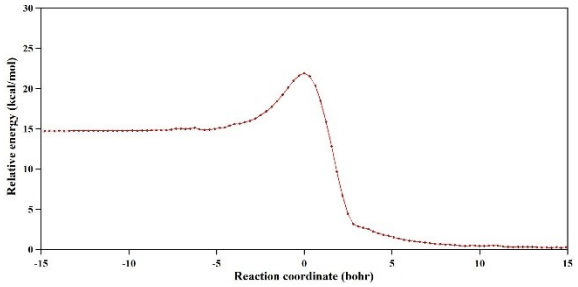

R6

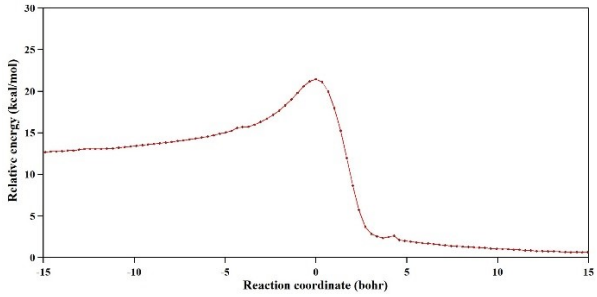

R7

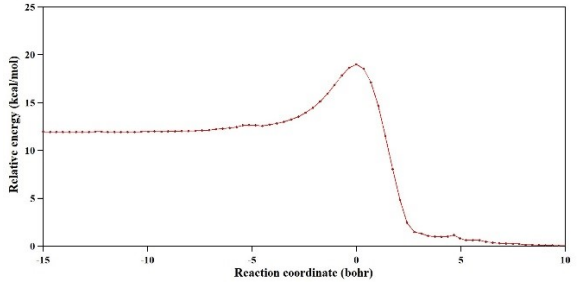

R8

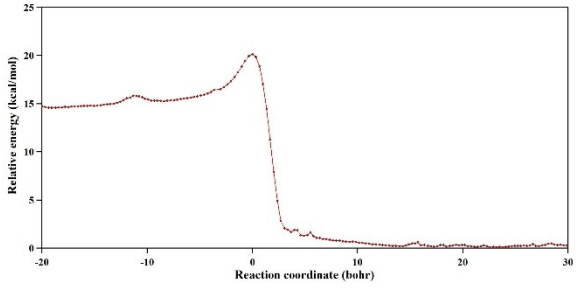

R9

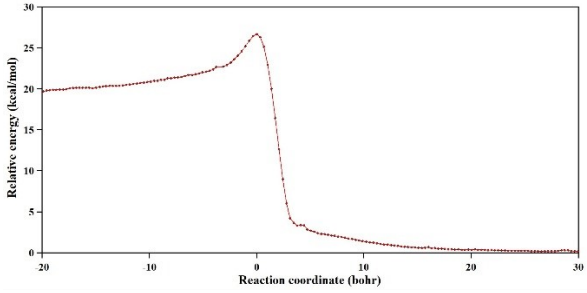

R10

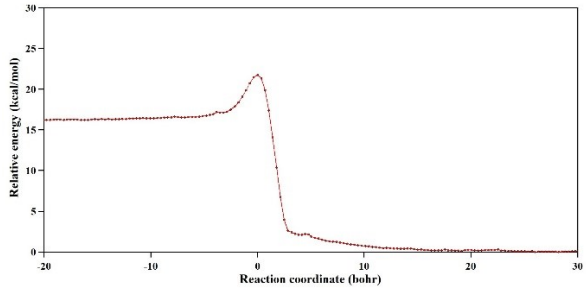

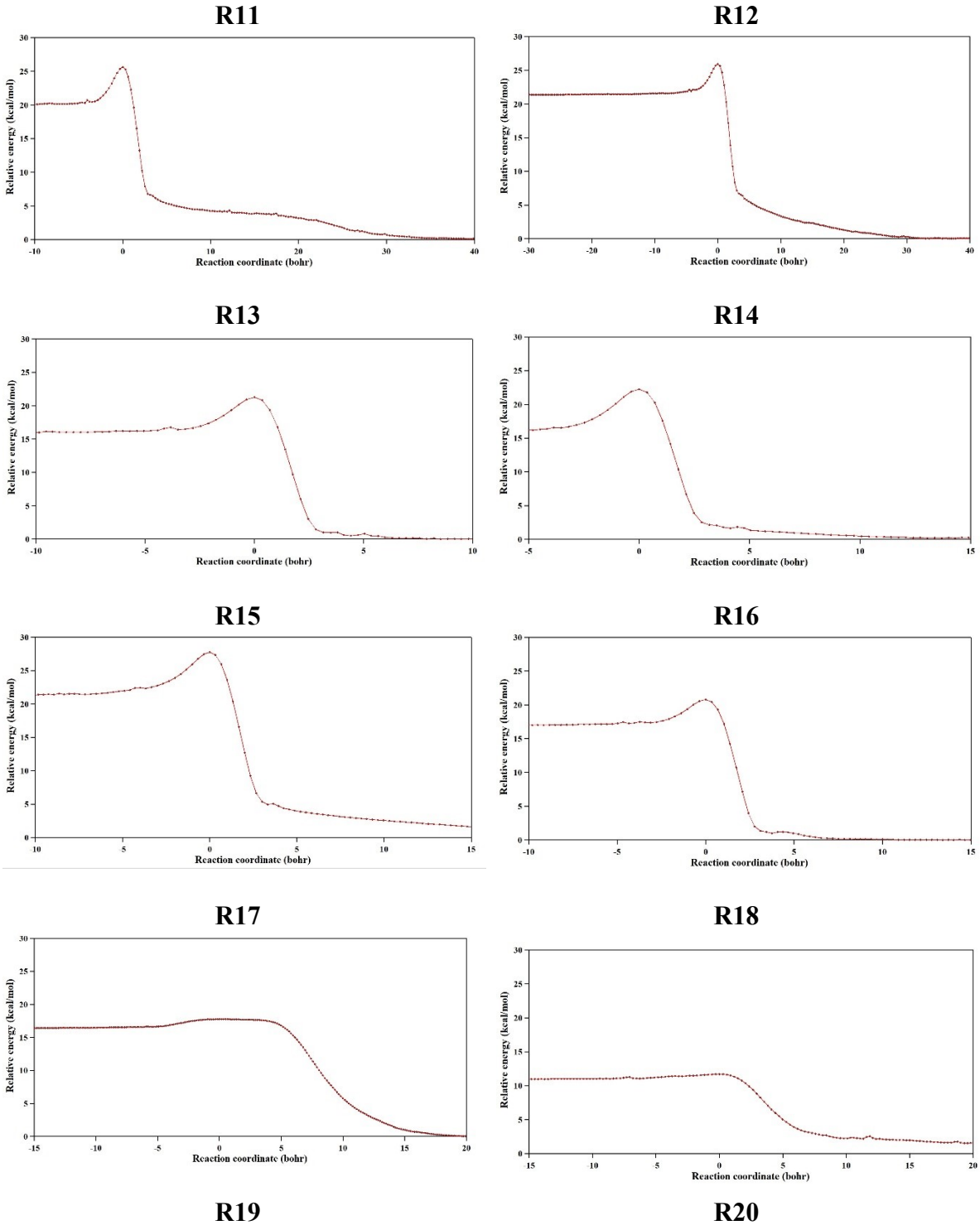

Figure S1. The IRC plots for the •OH initiated reactions of fenthion calculated at M06-2X/6-311++G(d,p) level of theory.

	REACTANT COMPLEX (RC)	TRANSITION STATE (TS)	PRODUCT COMPLEX (PC)
R1	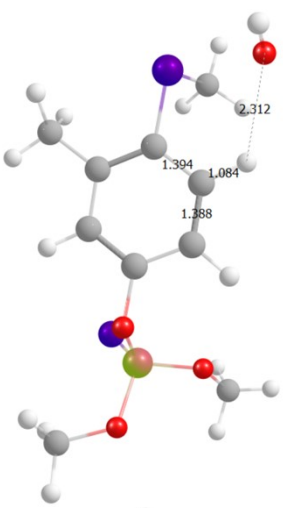	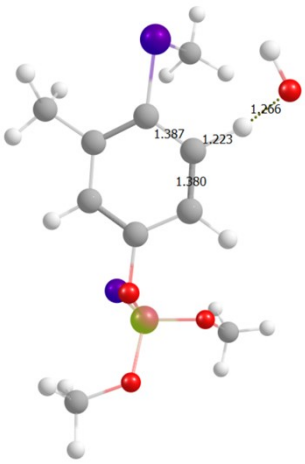	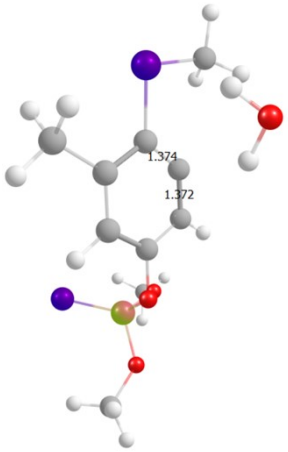
R2	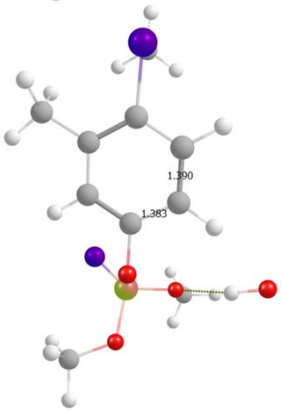	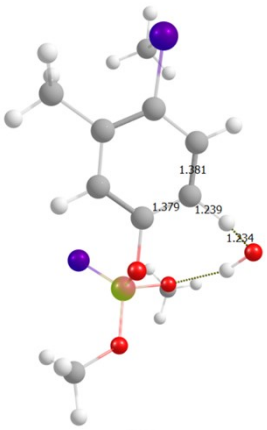	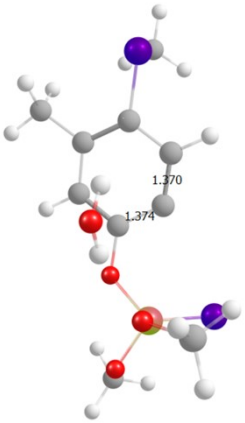
R3	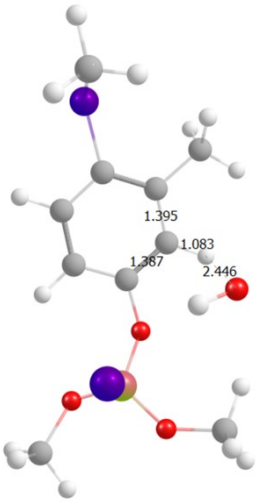	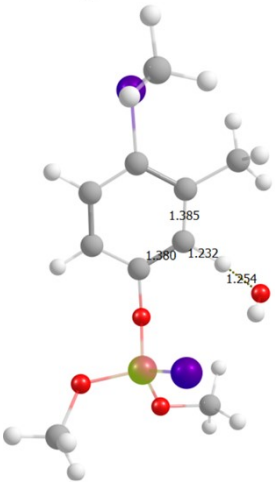	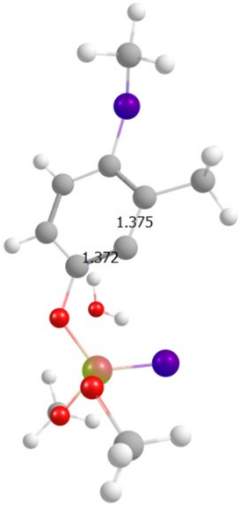

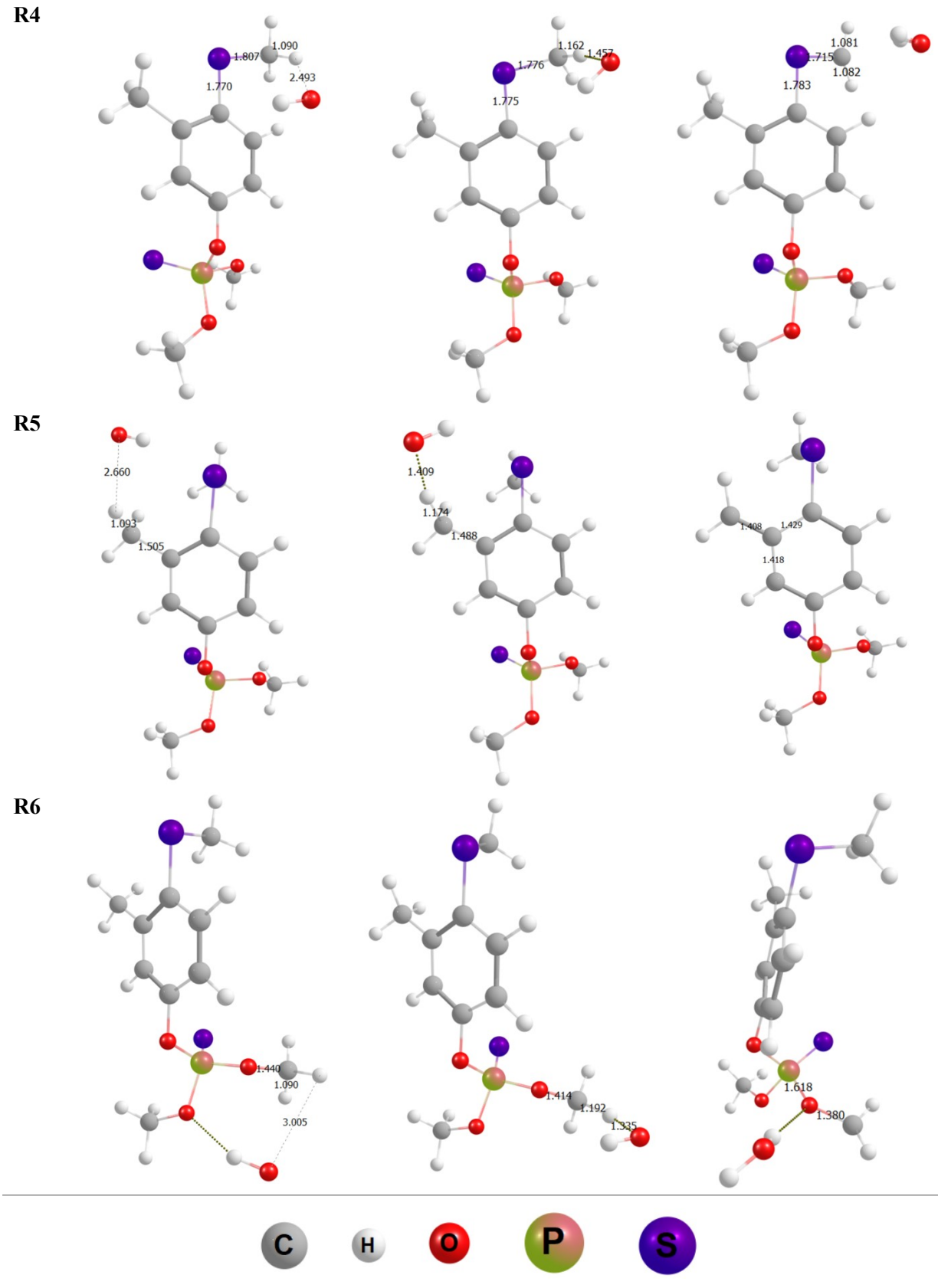

Figure S2. The geometry of reactive species involved in the H abstraction reaction of fenthion initiated by •OH optimized at M06-2X/6-311++G(d,p) level of theory.

	REACTANT COMPLEX (RC)	TRANSITION STATE (TS)	PRODUCT (P)
R7	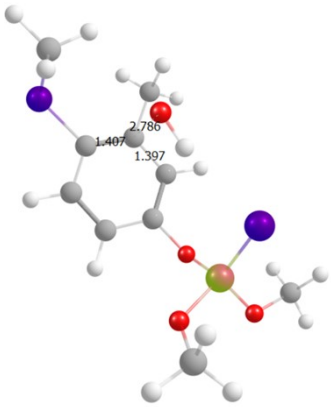	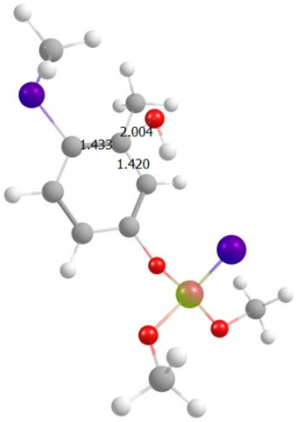	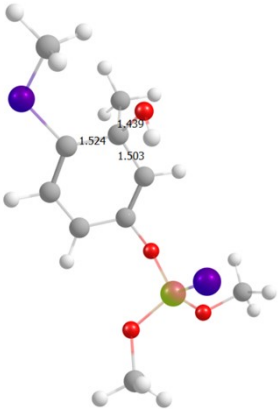
R8	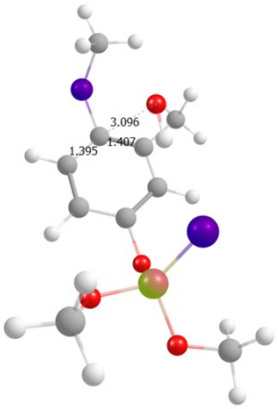	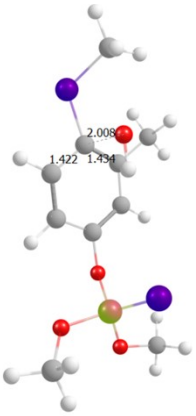	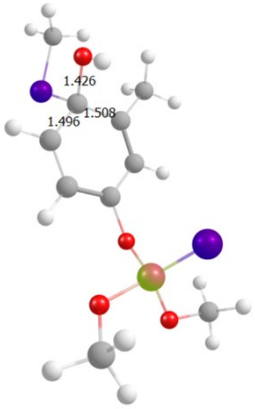
R9	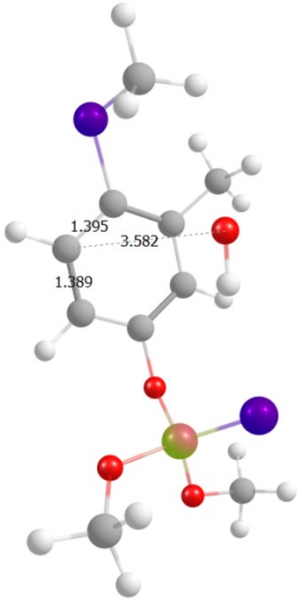	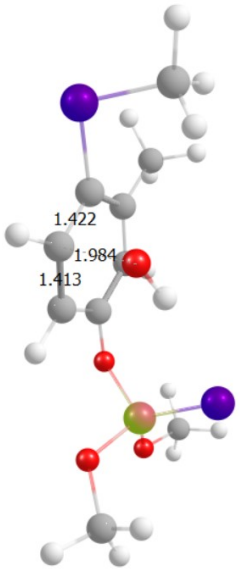	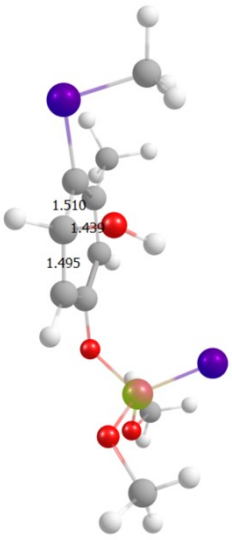

R10

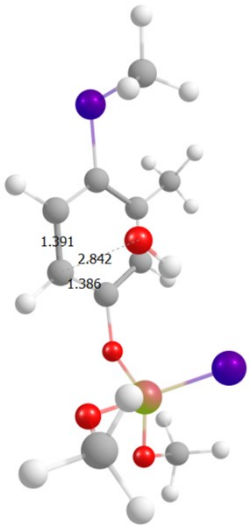
1.391
2.842
1.386

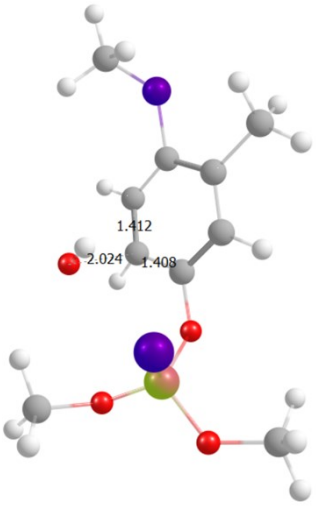
1.412
2.024
1.408

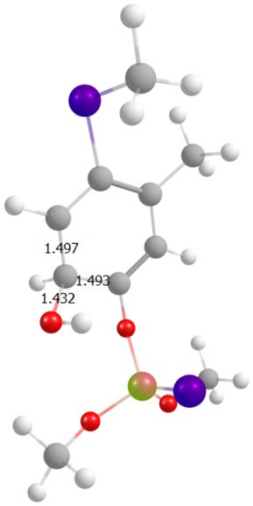
1.497
1.493
1.432

R11

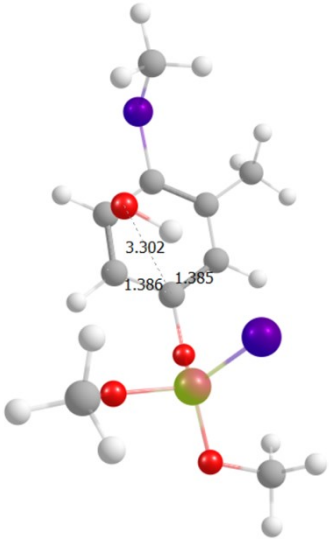
3.302
1.386
1.385

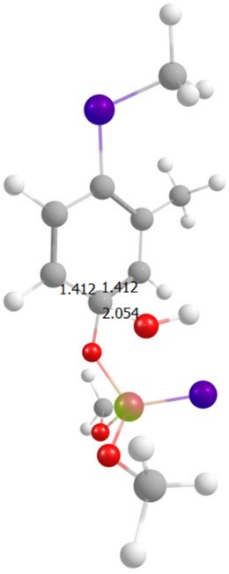
1.412
1.412
2.054

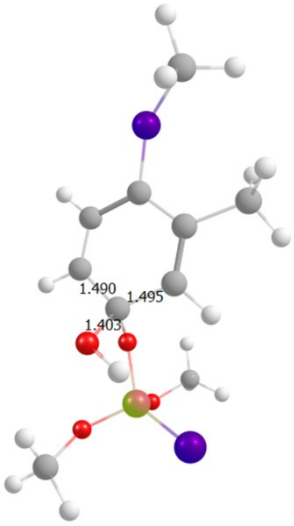
1.490
1.495
1.403

R12

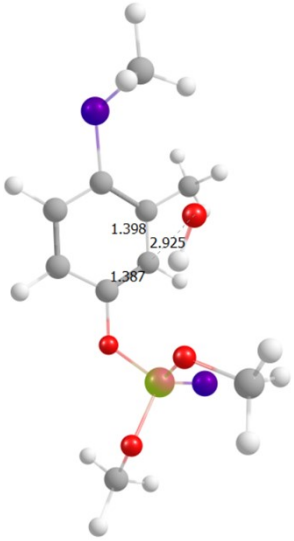
1.398
2.925
1.387

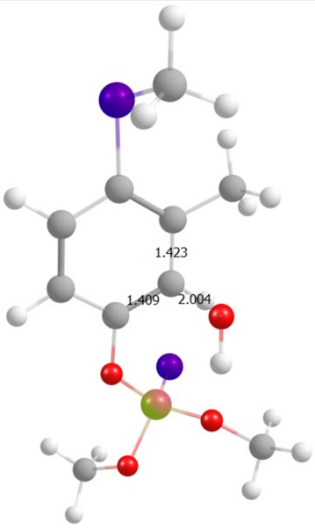
1.423
1.409
2.004

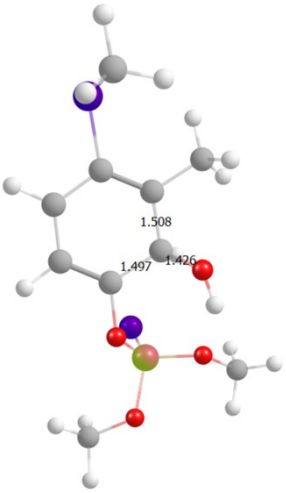
1.508
1.497
1.426

R13

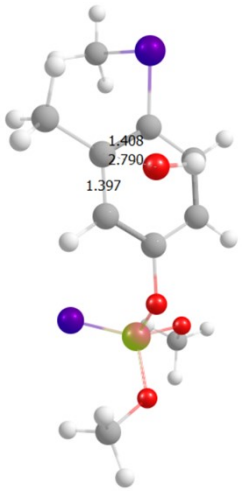
1.408
2.790
1.397

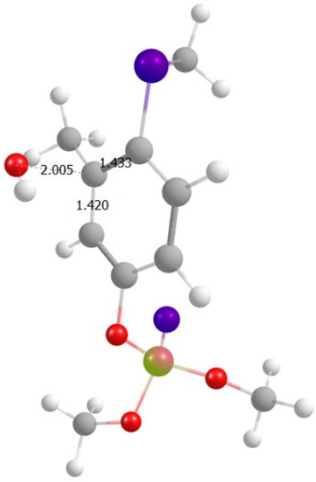
2.005
1.433
1.420

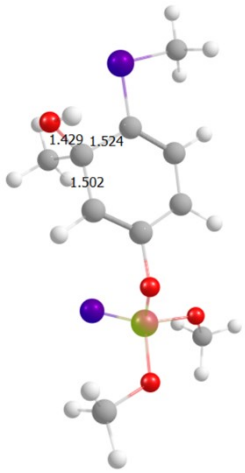
1.429
1.524
1.502

R14

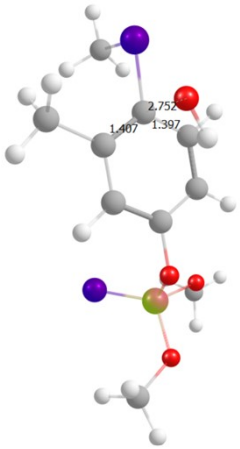
2.752
1.407
1.397

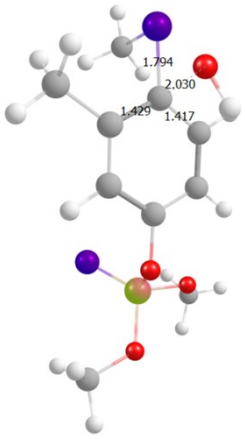
1.794
2.030
1.429
1.417

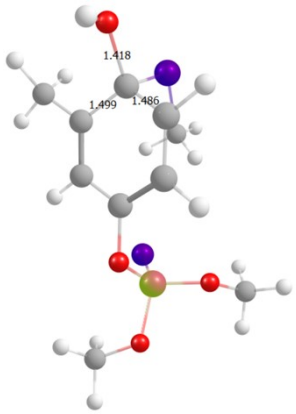
1.418
1.499
1.486

R15

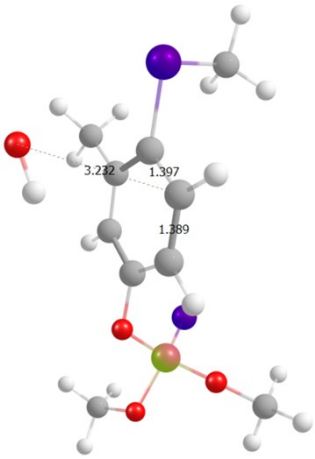
3.232
1.397
1.389

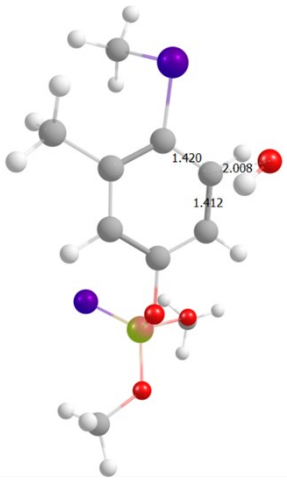
1.420
2.008
1.412

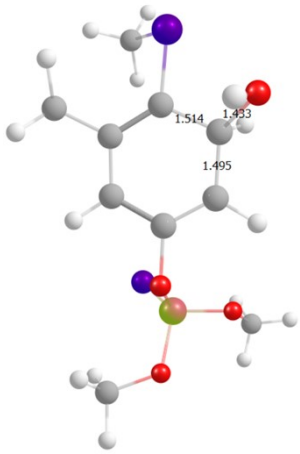
1.514
1.453
1.495

R16

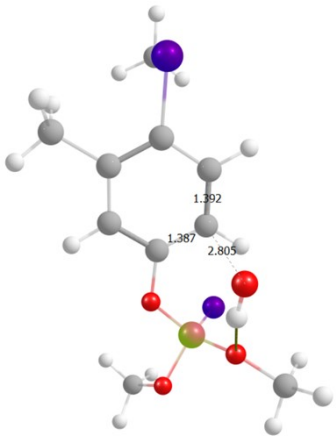
1.392
1.387
2.805

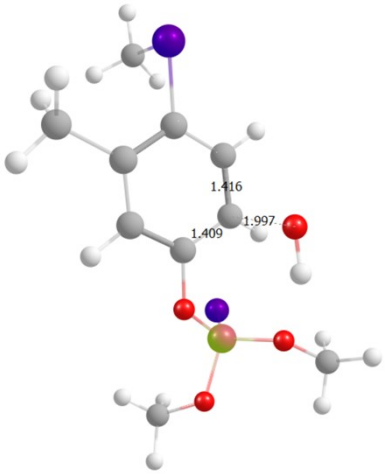
1.416
1.997
1.409

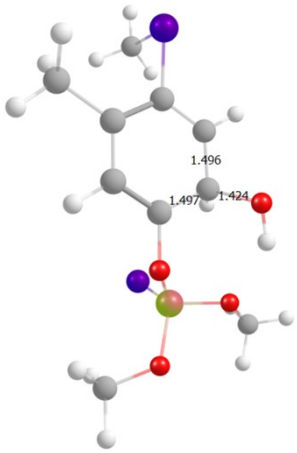
1.496
1.497
1.424

R17

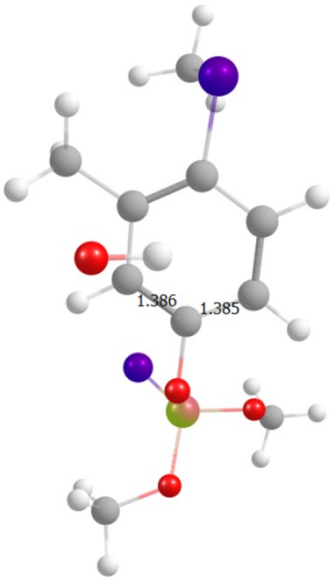
1.386
1.385

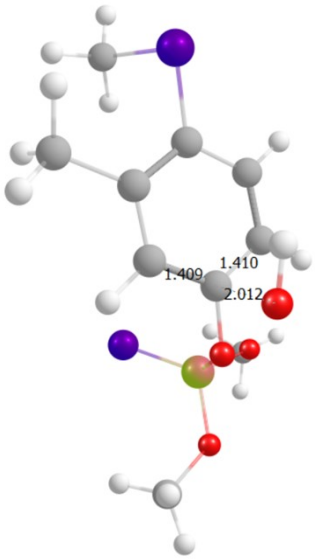
1.410
1.409
2.012

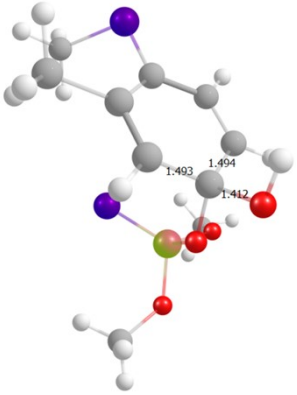
1.493
1.494
1.412

R18

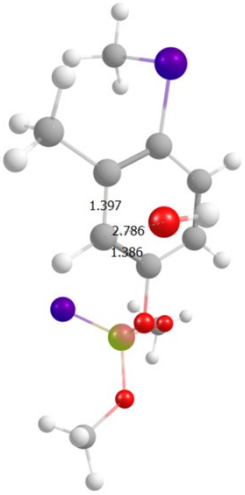
1.397
2.786
1.386

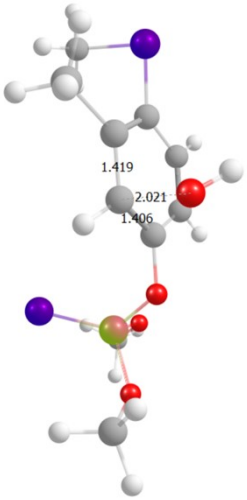
1.419
2.021
1.406

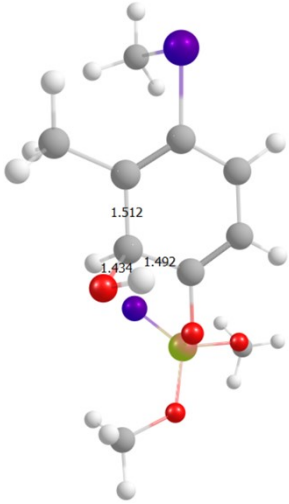
1.512
1.434
1.492

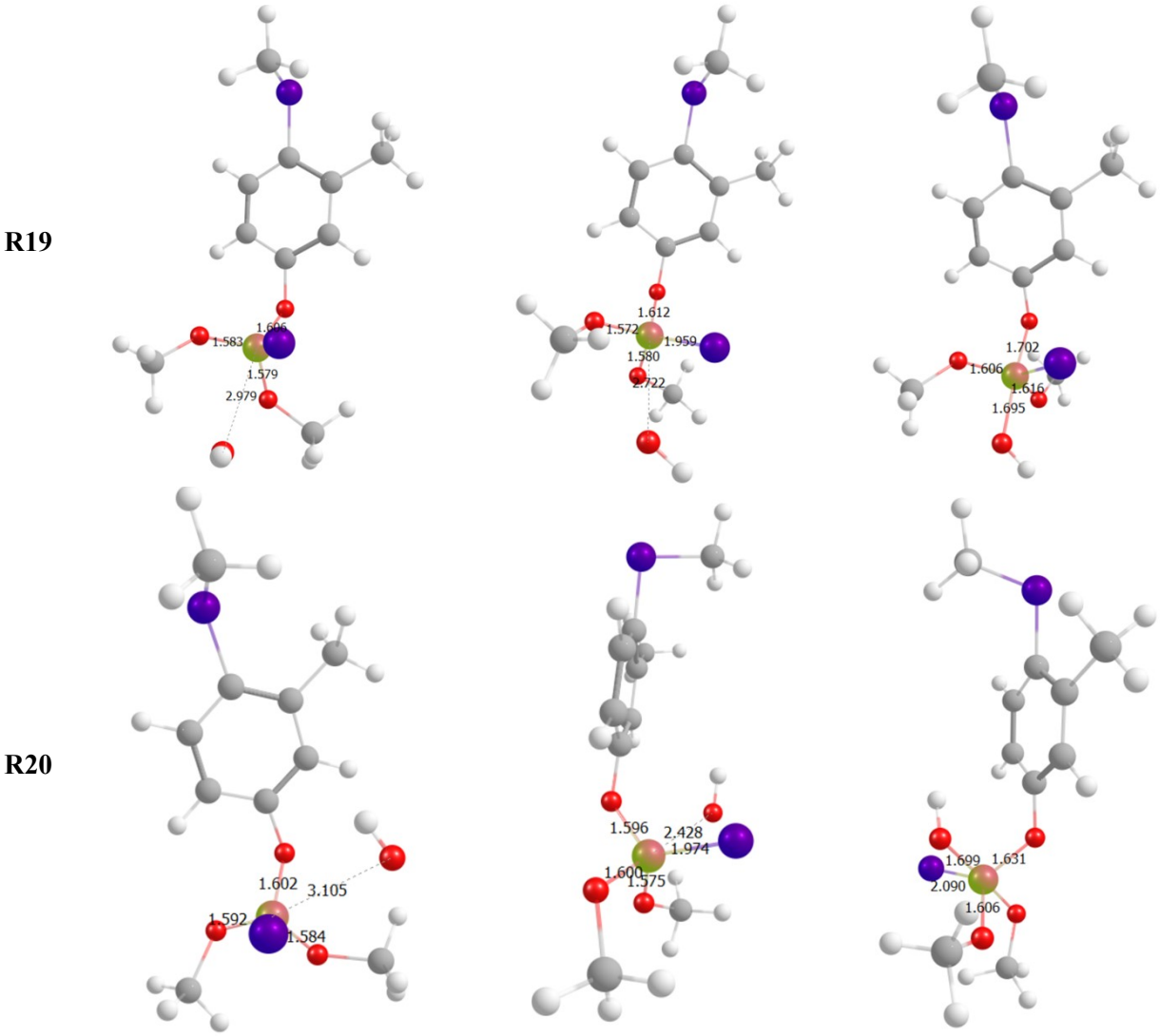

Figure S3. The geometry of reactive species involved in the •OH-addition reactions of fenthion optimized at M06-2X/6-311++G(d,p) level of theory.

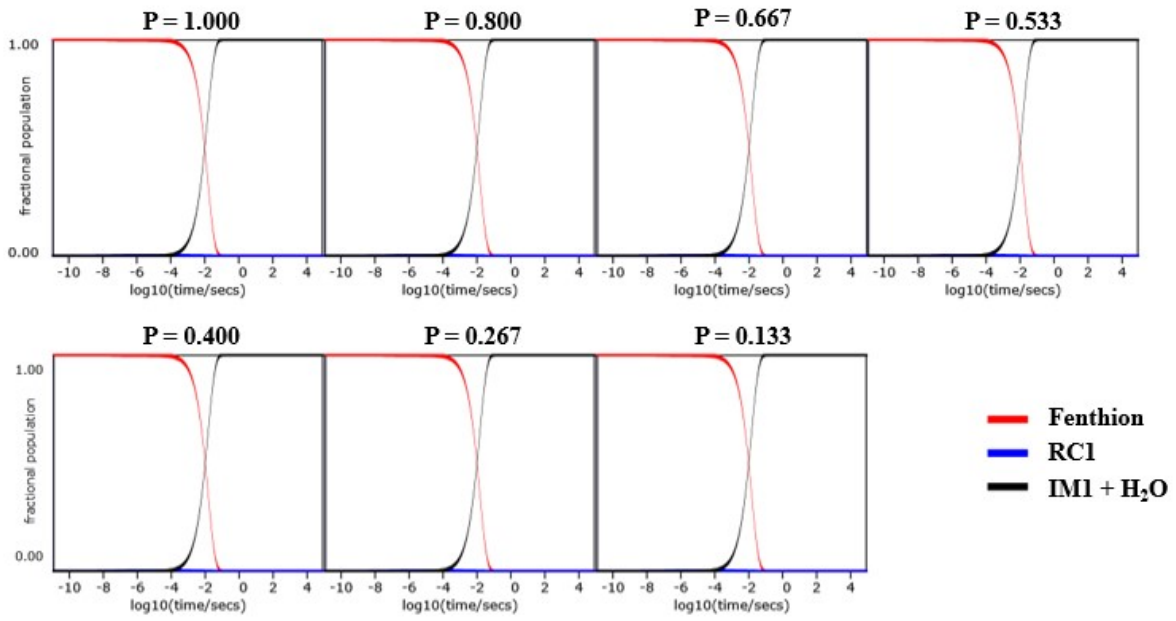

Figure S4. Time-dependent species population profiles for the reaction pathway R1 at 298 K, calculated at different pressures (P) using MESMER software employing RRKM theory. The pressure values are given in bar.

	REACTANT COMPLEX (RC)	TRANSITION STATE (TS)	PRODUCT (P)
S1FE	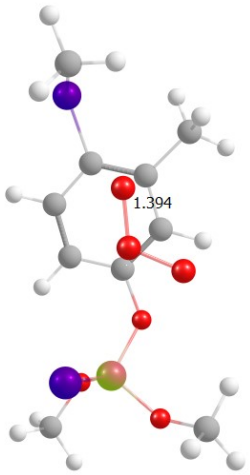	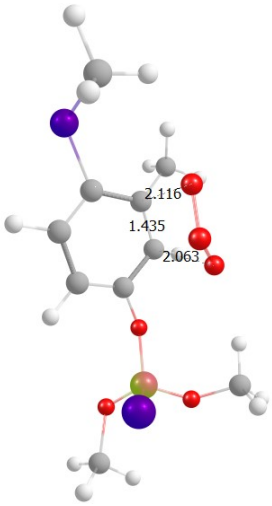	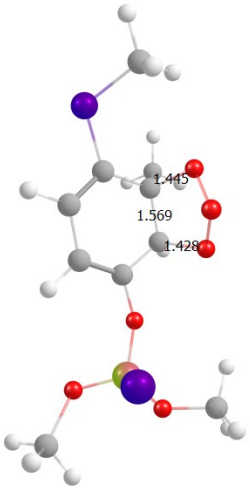
S1FX	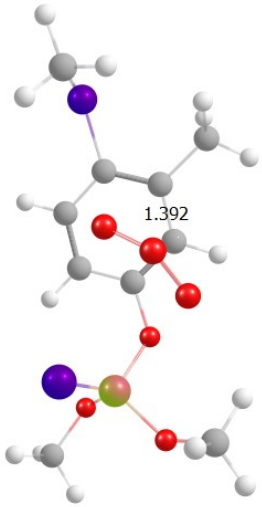	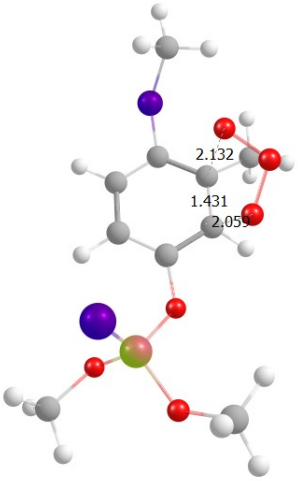	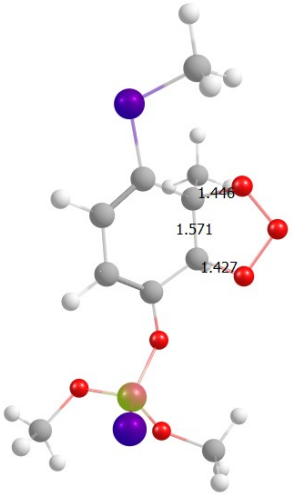
S1BE	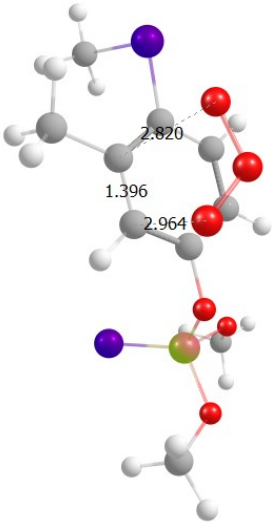	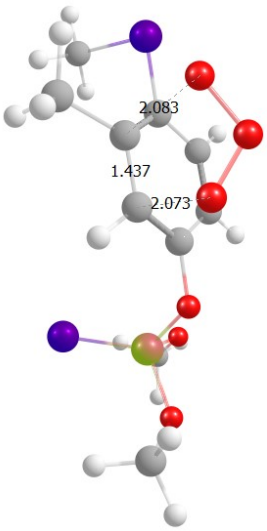	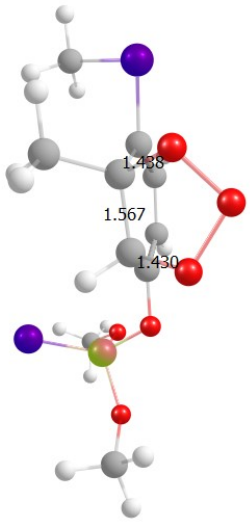

S1BX

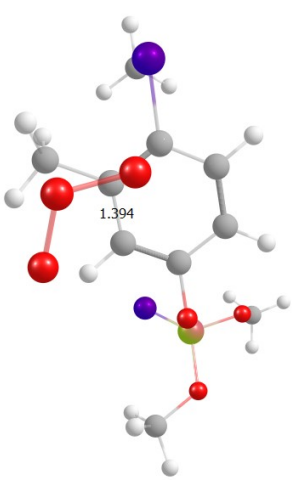

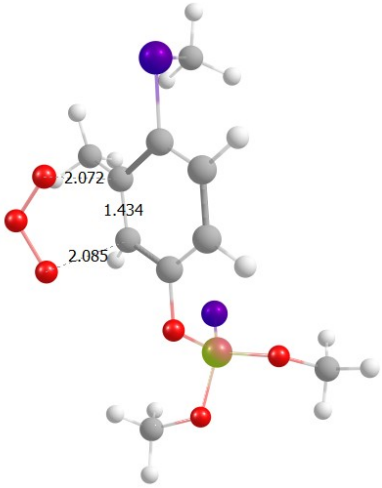

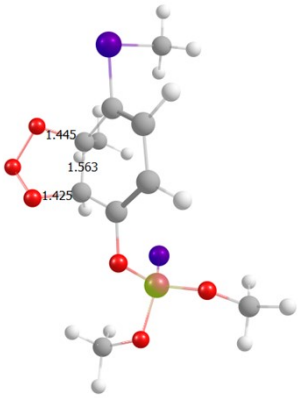

S2FE

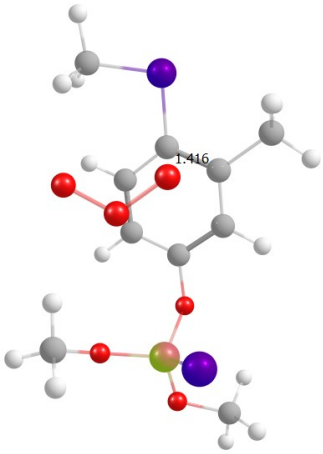

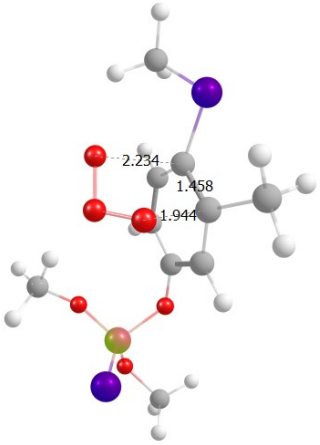

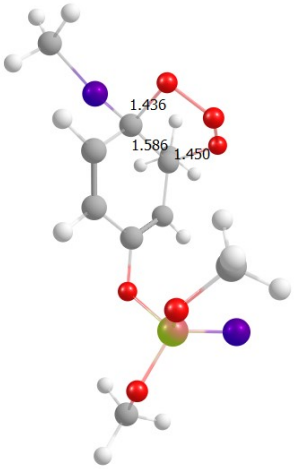

S2FX

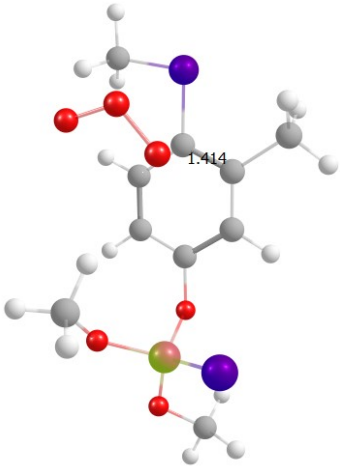

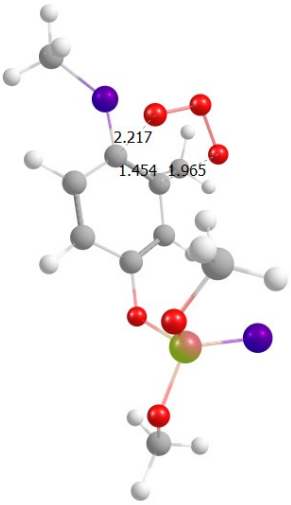

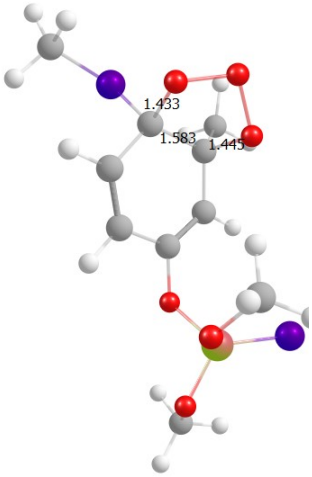

S2BE

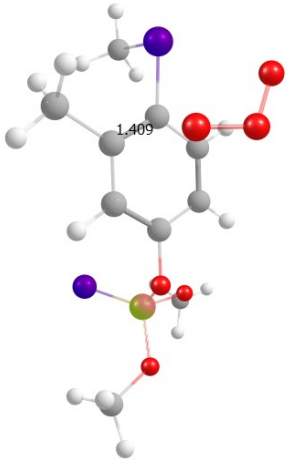

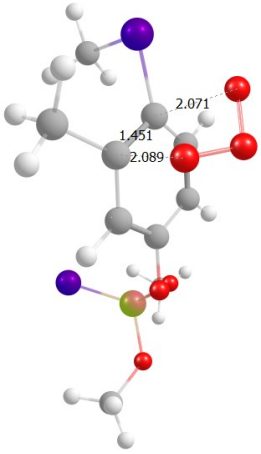

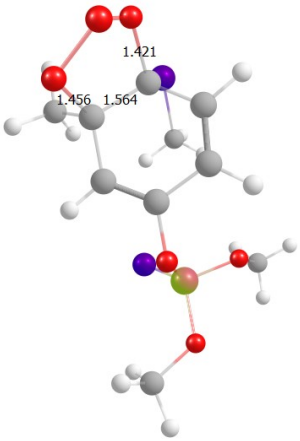

S2BX

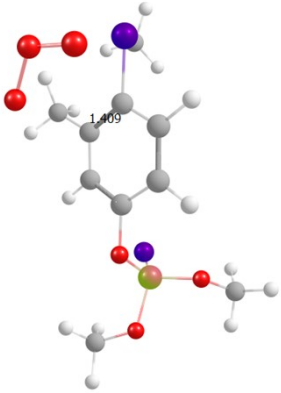

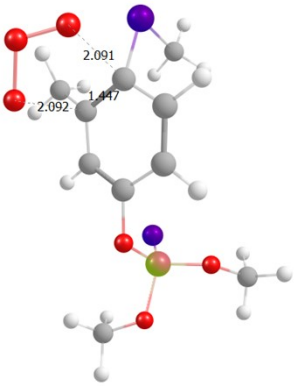

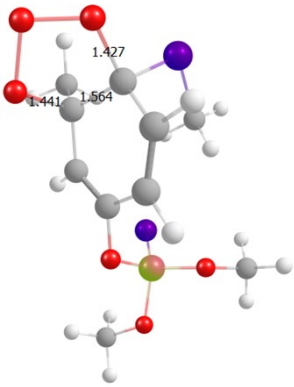

S3FE

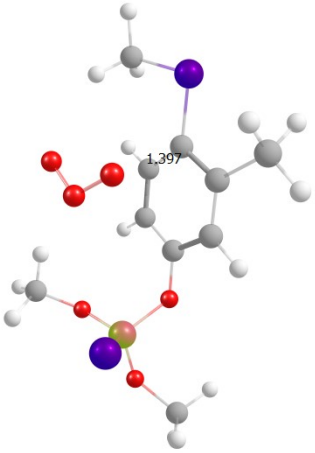

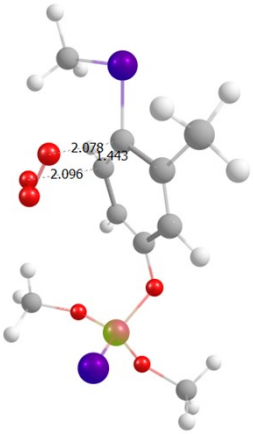

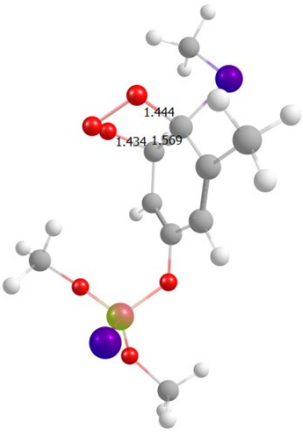

S3FX

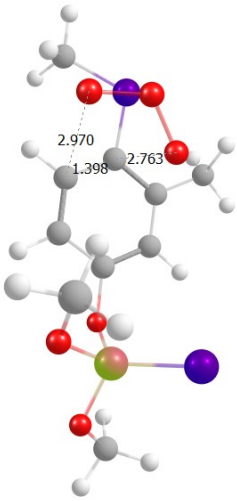

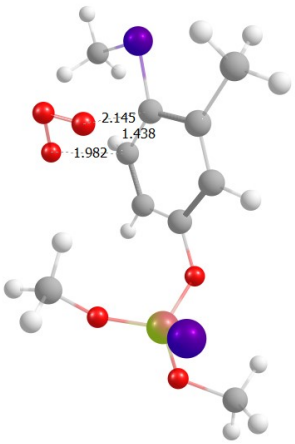

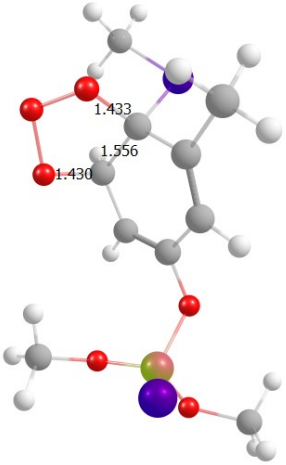

S3BE

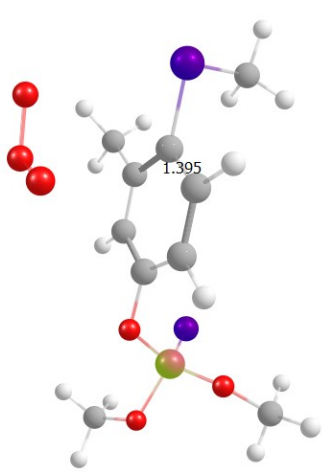

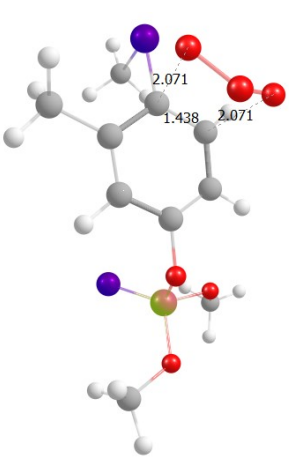

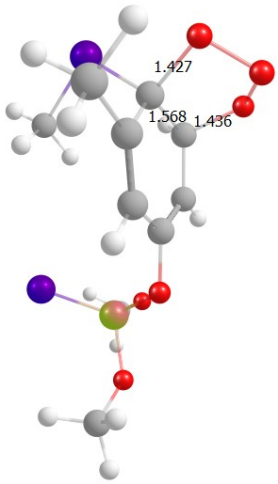

S3BX

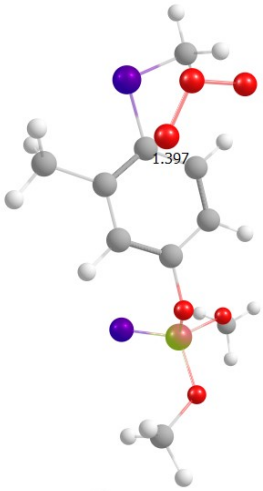

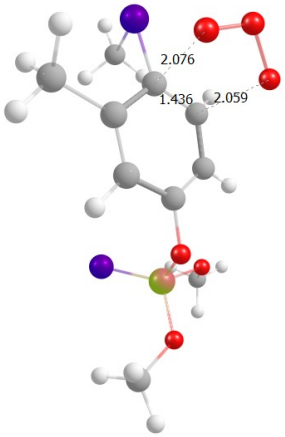

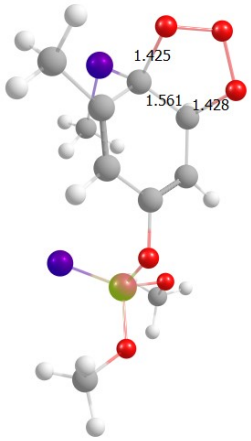

S4FE

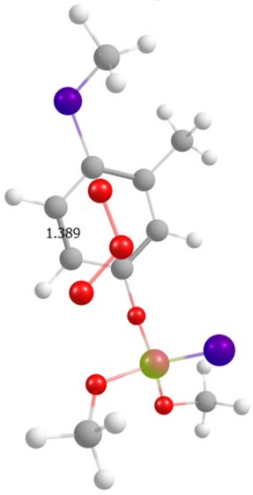

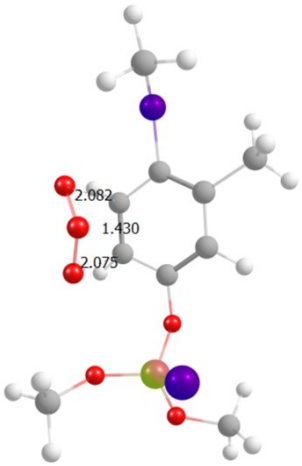

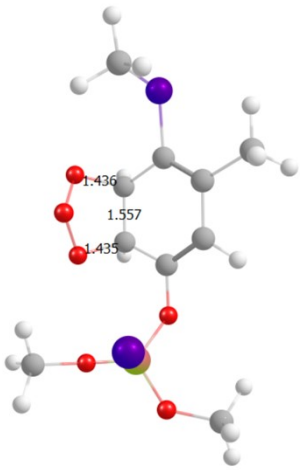

S4FX

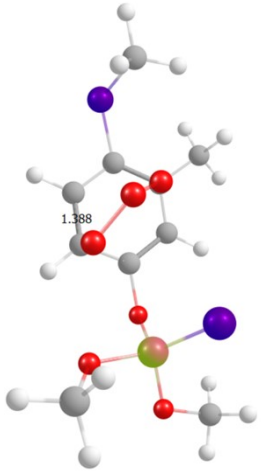

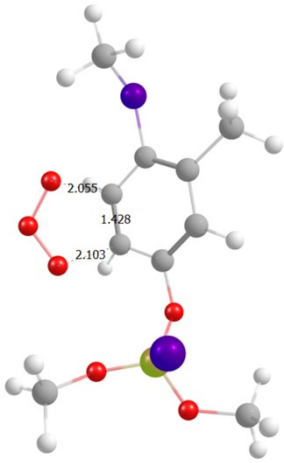

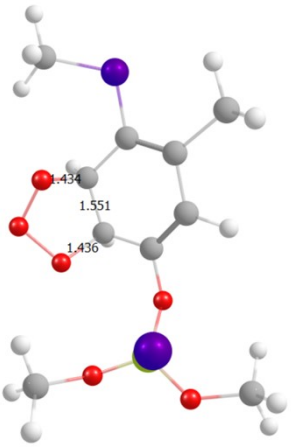

S4BE

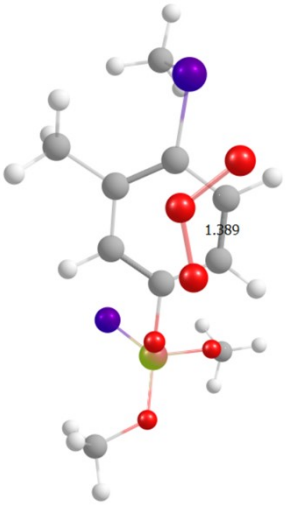

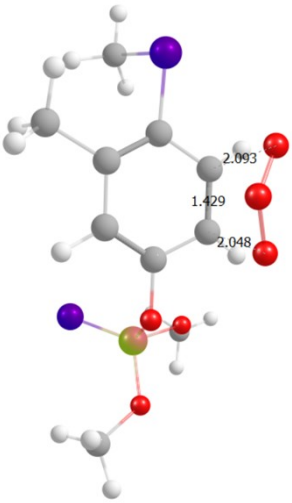

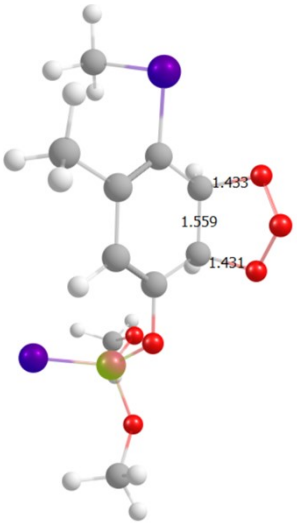

S4BX

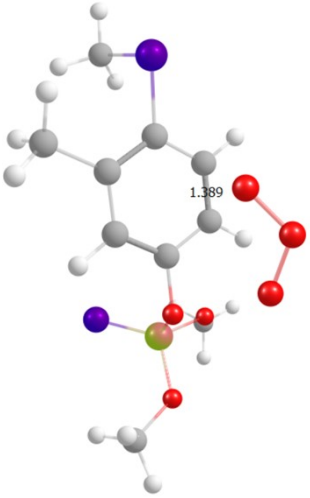

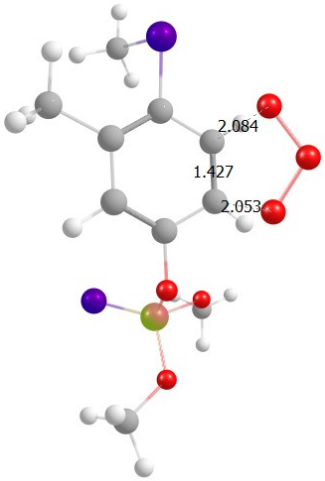

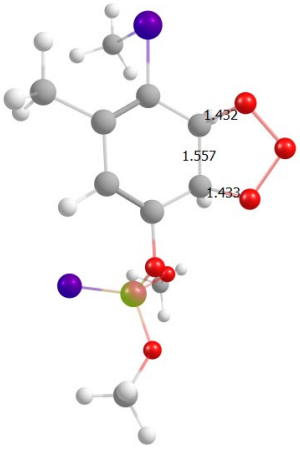

S5FE

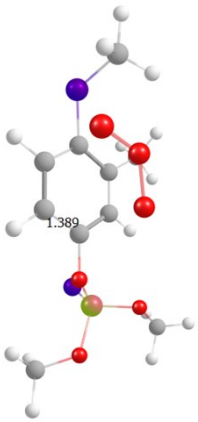

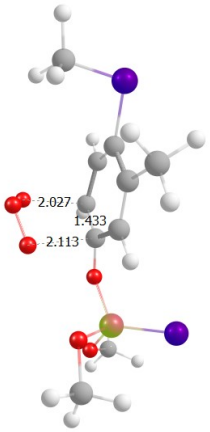

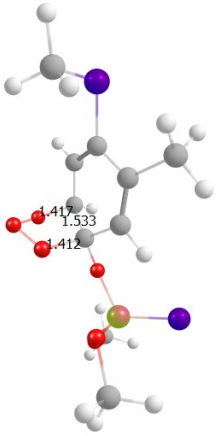

S5FX

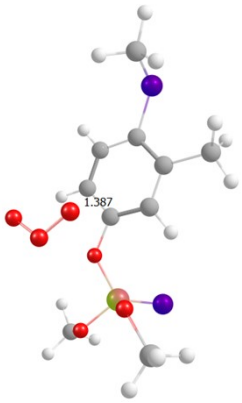

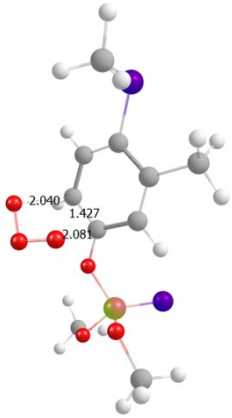

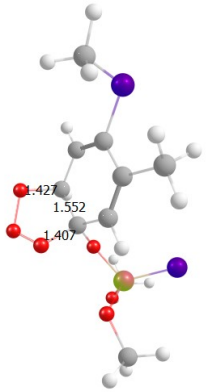

S5BE

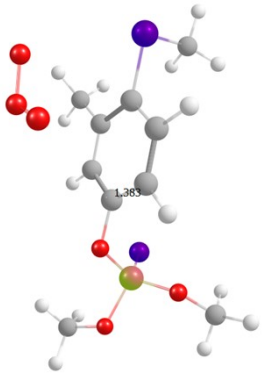

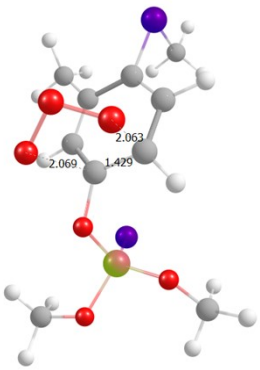

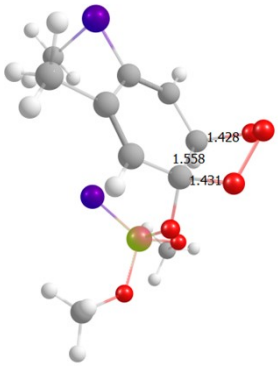

S5BX

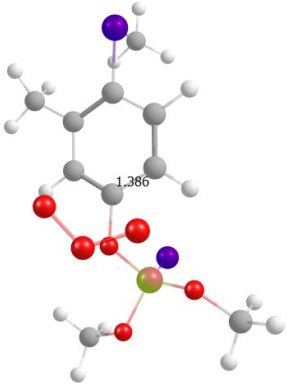

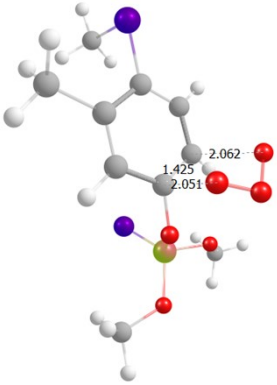

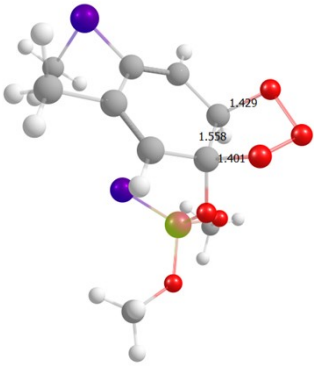

S6FE

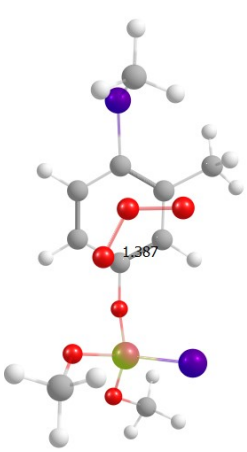

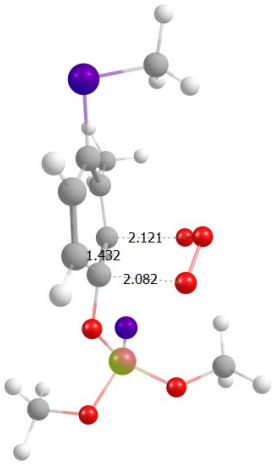

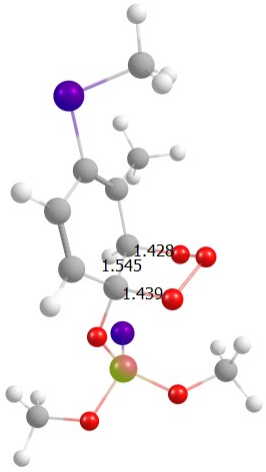

S6FX

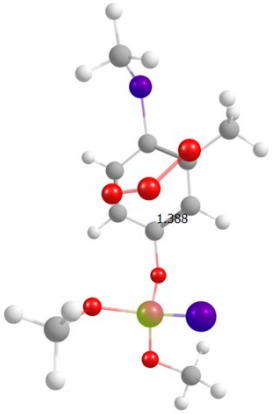

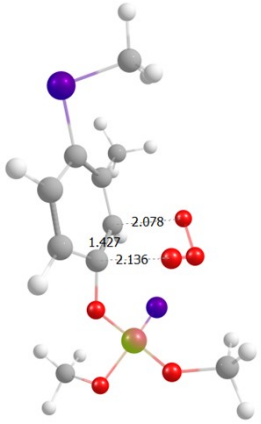

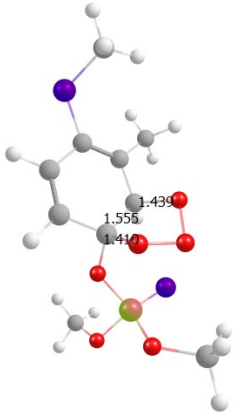

S6BE

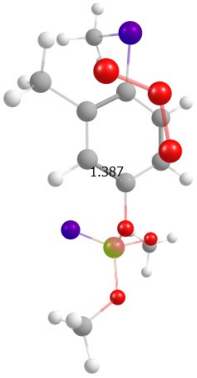

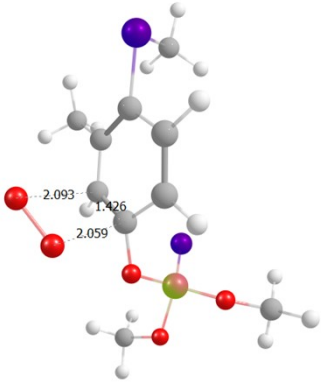

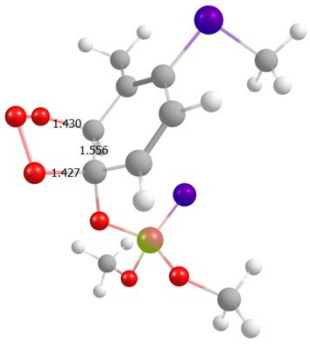

S6BX

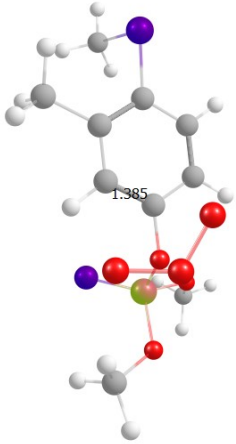

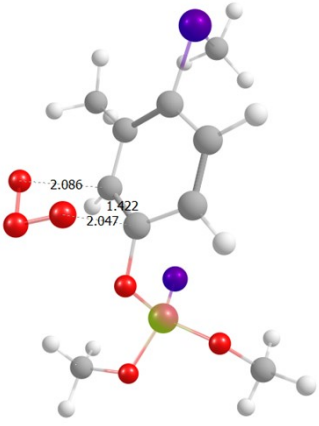

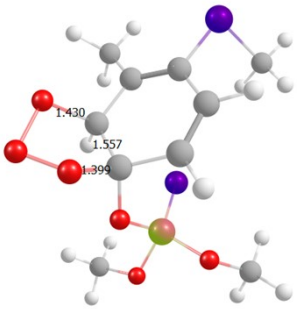

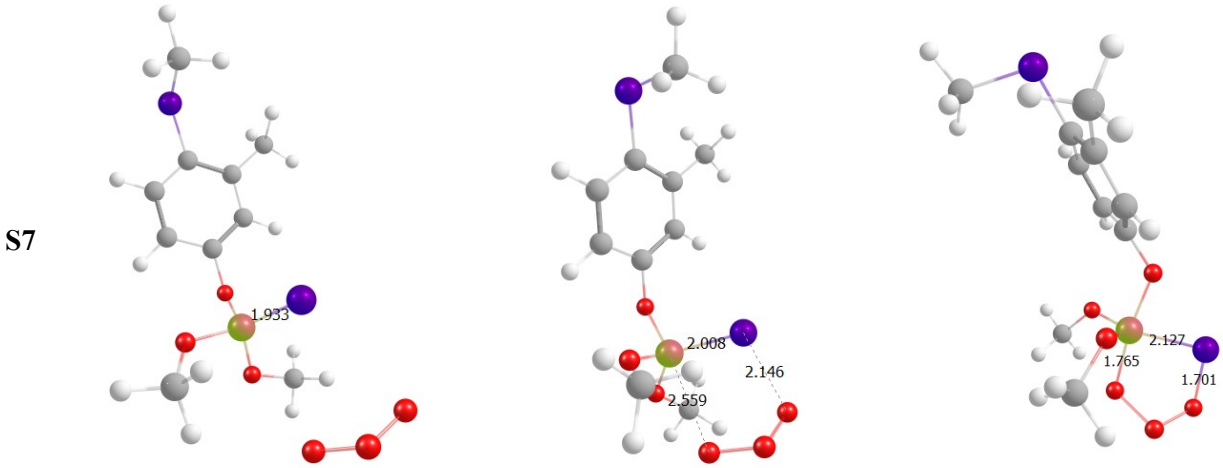

Figure S5. The geometry of reactive species involved in the O_3-initiated reactions of fenthion optimized at M06-2X/6-311++G(d,p) level of theory.